Journal of Power Sources 248 (2014) 900–904

Contents lists available at ScienceDirect

Journal of Power Sources

journal homepage: www.elsevier.com/locate/jpowsour

Short communication

New in-situ neutron diffraction cell for electrode materials

Jordi Jacas Biendicho [a,b,*], Matthew Roberts [c], Colin Offer [a], Dag Noréus [b], Erika Widenkvist [d], Ronald I. Smith [a], Gunnar Svensson [b], Kristina Edström [c], Stefan T. Norberg [e], Sten G. Eriksson [e], Stephen Hull [a,*]

[a] The ISIS Facility, STFC Rutherford Appleton Laboratory, UK
[b] Department of Material and Environmental Chemistry, Stockholm University, Sweden
[c] Department of Materials Chemistry, Uppsala University, Sweden
[d] Nilar Svenska AB, Gavle, Sweden
[e] Department of Chemical and Biological Engineering, Chalmers University of Technology, Sweden

HIGHLIGHTS

- A novel neutron diffraction cell for in-situ studies of electrode materials is presented.
- The cell design maximises the amount of electrode material exposed to the neutron beam.
- Neutron diffraction patterns collected in-situ using deuterated electrolyte show a good signal-to-noise ratio.
- The electrochemical behavior of a typical Ni–MH battery has been reproduced using the new cell.
- Atomic positions, isotropic thermal parameters and deuterium site occupancies were refined for the MH charged phase (β-phase).

ARTICLE INFO

Article history:
Received 8 August 2013
Received in revised form
27 September 2013
Accepted 30 September 2013
Available online 11 October 2013

Keywords:
Neutron diffraction
In-situ electrochemical cell
Electrode materials
Ni–MH battery
Secondary batteries

ABSTRACT

A novel neutron diffraction cell has been constructed to allow in-situ studies of the structural changes in materials of relevance to battery applications during charge/discharge cycling. The new design is based on the coin cell geometry, but has larger dimensions compared to typical commercial batteries in order to maximize the amount of electrode material and thus, collect diffraction data of good statistical quality within the shortest possible time. An important aspect of the design is its modular nature, allowing flexibility in both the materials studied and the battery configuration. This paper reports electrochemical tests using a Nickel-metal-hydride battery (Ni-MH), which show that the cell is able to deliver 90% of its theoretical capacity when using deuterated components. Neutron diffraction studies performed on the Polaris diffractometer using nickel metal and a hydrogen-absorbing alloy (MH) clearly show observable changes in the neutron diffraction patterns as a function of the discharge state. Due to the high quality of the diffraction patterns collected in-situ (i.e. good peak-to-background ratio), phase analysis and peak indexing can be performed successfully using data collected in around 30 min. In addition to this, structural parameters for the β-phase (charged) MH electrode obtained by Rietveld refinement are presented.

1. Introduction

Electrochemical devices such as secondary batteries are extensively employed in many applications, with considerable research effort currently directed towards their future use as environmentally friendly sources of electrical power within the automotive industry. To achieve better battery technologies, with improved power densities and more rapid charge/discharge times, we require new materials to fulfil the key roles of electrodes and electrolyte. In turn, it is essential to perform detailed characterisation of any candidate

* Corresponding authors. The ISIS Facility, STFC Rutherford Appleton Laboratory, UK.
E-mail address: jordi.jacas@stfc.ac.uk (J.J. Biendicho).

0378-7753
http://dx.doi.org/10.1016/j.jpowsour.2013.09.141

materials, to identify those factors which promote (or hinder) their electrochemical reactions.

For analysis of the crystal structure of battery materials, neutron diffraction often has an advantage over its X-ray counterpart owing to its increased sensitivity to the location of the mobile species, which are generally light ions such as Li^+ and H^+. Indeed, neutron diffraction has been extensively employed to probe the preferred sites for such ions within battery electrode materials, using samples extracted by dismantling a battery at a chosen stage of charge/discharge and examining the various components ex-situ (for recent examples, see [1,2]). However, since the pioneering work of Bergstrom et al. [3], the past decade has seen an increased interest in the development of new in-situ electrochemical cells built to enable experiments to be performed under realistic operating conditions. Such experiments performed in-situ on a neutron diffractometer can give a more comprehensive insight into the structural processes at the electrodes than the commonly used ex-situ experiments since, for example, some of the reaction products that occur during the electrochemical reactions are only stable during battery operation [4].

The quality of the structural information that may be obtained from a particular in-situ cell is dependent on its design and components. In general, the following criteria apply

(i) The typical incident flux at a neutron source is relatively low (compared to synchrotron X-ray sources) so it is advantageous to use relatively large ($\sim cm^3$) sized samples, if possible.
(ii) Neutrons can easily penetrate metal containers, but these can still produce additional Bragg peaks in the measured diffraction pattern.
(iii) If studying the locations of H within the battery material, it is advisable to replace H with the isotope D if possible, to exploit its higher scattering power and significantly lower incoherent scattering section.
(iv) To reduce the level of incoherent scattering, the amount of H in other components within the cell should be minimised.
(v) The electrochemical performance of the in-situ cell for neutron diffraction studies should be comparable to that of the 'real' battery in order to ensure that the results obtained are directly relevant to technological applications.

The original cell reported by Bergstrom et al. [3] and further developed by Berg et al. [5] comprised a Pyrex tube which was gold-plated on its inner surface and filled with a mixture of electrode material and electrolyte. This configuration allowed the in-situ investigation of a substantial amount of electrode material. However, the cell suffered from slow kinetics. A new approach has been reported by Roberts et al. [6] recently. The new cell contains a wound laminate made up of cathode, anode, current collectors and separators. With this arrangement, it has been shown that cycling a Li-ion battery at fast current rates is possible, whilst maintaining a good peak-to-background ratio in the neutron diffraction pattern collected (provided that deuterated components are used). A similar custom-built cell has been designed by Sharma et al. [7–10], in order to reproduce commercial Li-batteries with H-free components.

The use of in-situ neutron diffraction has not been limited only to Li-ion batteries. Latroche et al. [11–14] used specially designed silica cells to characterize metal hydride (MH) electrodes in-situ. In spite of the large background contribution observed in these cells due to the silica container, the effect of cobalt content in $MmNi_{4.3-x}Mn_{0.3}Al_{0.4}Co_x$ where Mm = mischmetal (x = 0.36 and 0.69) electrodes was reported [13]. In-situ studies indicated that the main limiting factor that governs the kinetics of these materials was the α- to β-phase transformation that takes place at the electrodes during charge/discharge [12]. The same cell was used to monitor the two-phase mechanism in the nickel hydroxide electrode in-situ [15]. Alternatively, another cell has been built to enable characterisation of MH electrodes in-situ [16] but its design limitations meant that electrochemical studies were restricted to slow rates.

In addition to cylindrical cells, the coin cell geometry has also been adapted for in-situ neutron diffraction experiments. Coin cell batteries of a few centimeters in diameter are commonly used in laboratory facilities to test electrode materials and the same design may be applied, on a larger scale, to conduct in-situ characterisation. A cell based on this configuration was presented by Novak et al. and tested using two electrodes $LiNiO_2$ [17] and $Li_4Ti_5O_{12}$ [18]. The cell has been upgraded recently [19] and tested on the D20 powder neutron diffractometer at ILL, France. In the original cell, electrodes were electrochemically cycled at relatively slow rates. However, with the new upgrade, the rates are improved while maintaining a good peak-to-background ratio in the neutron diffraction patterns if deuterated components are used.

In this paper, we present the design of a new cell for studying electrode materials in-situ by neutron diffraction. In addition to the criteria listed above, the cell design is deliberately modular, allowing different materials and configurations to be used dependent on the type of battery technology of interest and the specific aims of a particular experiment. Its use is demonstrated using neutron diffraction data collected in-situ which allowed the changes at the negative electrode (MH) in an Air–MH battery to be monitored, and in addition enabled the crystal structure of the charged MH electrode or β-phase to be analyzed using the Rietveld method [20].

2. Cell design

The design of the in-situ electrochemical cell is based on the coin cell geometry and is constructed of a number of circular disk-shaped components with an outer diameter of 15 cm. The cell is constructed by stacking different components (described in more detail below), so that different cell configurations can be assembled depending on the type of battery under investigation, or to maximize the amount of electrode material exposed to the neutron beam (in order to increase the intensity of the Bragg peaks from the electrode material compared to the construction materials). The cell is, therefore, flexible in the sense that different configurations may be assembled for experiments in-situ.

For a battery configuration (1 working electrode, 1 counter electrode and 1 separator), 2 windows and 1 separator modules are required. This configuration may be extended to a more complex one or two half-cells configuration by adding an extra separator and window. For the latter, Fig. 1(a) illustrates a 3D model of an assembled cell, whilst Fig. 1(b) shows the cell stacking sequence and alignment with respect to the incident neutron beam. The window is a nickel plate (99.99% purity, 1 mm thick) with a 40 mm high by 20 mm wide aperture to allow passage of the neutron beam, Figs. 1b-3. Next to this plate is a thin Ni metal sheet, whose thickness is minimized (typically to around 0.1 mm) in order to reduce the unwanted scattering as the neutron beam passes through it. This sheet also holds the electrode material and simultaneously acts as a current collector. The second module is used to house the separator, Fig. 1b-5, and is constructed from a 2 mm thick disk of polyoxymethylene, this material being chosen for its chemical resistance to the most commonly used electrolytes. The central aperture is also 40 mm high and 20 mm wide, to allow space for the electrode material and separator film. O-rings are used between each module to avoid leakage of the electrolyte. The

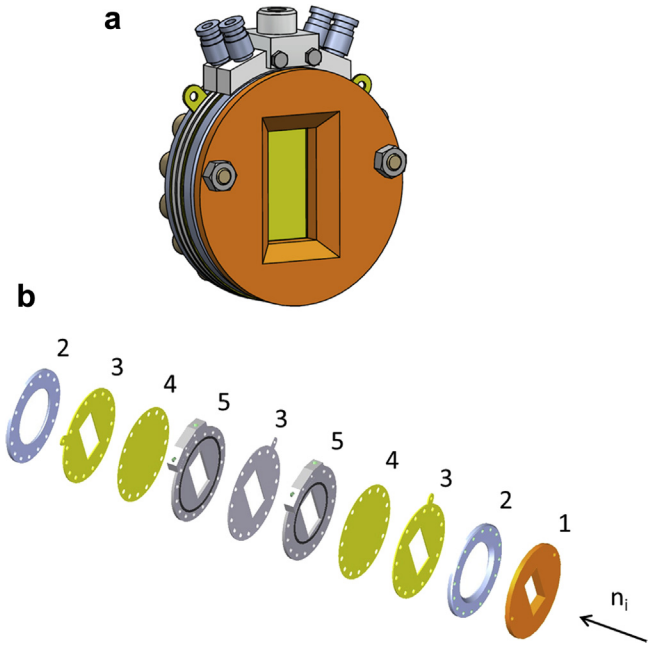

Fig. 1. (a) A 3D diagram of the assembled cell and (b) sketch of the cell components and their positions with respect to the incident neutron beam (1) is the boron nitride shield (2) alloy clamp rings (3) window (4) thin metal sheet and (5) separator.

separator disk has two channels from the inside void to fittings on the outside of the cell, to allow remote filling of the inner space with liquid electrolyte and/or release of gases evolved during the charge/discharge reactions. Two stainless steel alloy clamp rings on either side of the cell allow the cell to be clamped tight using 16 polyetheretherketone (PEEK) screws, chosen for their insulating character in order to avoid electrical short circuits. Finally, a boron nitride shield is located on the front of the cell as shown in Fig. 1b-1, exploiting the high thermal neutron absorption cross-section of boron (767 b at a neutron wavelength of 1.8 Å) to provide effective collimation of the incident/scattered neutron beam.

The design of the in-situ cell has been optimized to match the dimensions and scattering geometry of the high count rate Polaris powder diffractometer [21] at the ISIS spallation neutron source, STFC Rutherford Appleton Laboratory, UK, though with minor modifications it could readily be used on other pulsed neutron sources. A particular advantage of powder diffraction instruments at pulsed sources is their ability to collect diffraction patterns in detector banks at fixed scattering angles using the neutron time-of-flight method, thus avoiding the need for access to a wide range of scattering angles that characterizes powder diffractometers with fixed incident wavelength built at steady state (reactor) neutron sources. In the case of Polaris, the high intensity neutron beam (of dimensions 4 cm high × 2 cm wide) strikes the cell as shown in Fig. 1(b), which allows diffraction data to be collected in the detector banks at backscattering angles ($135° < 2\theta < 168°$, $d_{max} = 2.7$ Å, $\Delta d/d = 0.30\%$) and the two banks at lower angles ($40° < 2\theta < 67°$, $d_{max} = 7$ Å, $\Delta d/d = 0.86\%$ and $19° < 2\theta < 34°$, $d_{max} = 8.7$ Å, $\Delta d/d = 1.5\%$). In the following section we provide examples of the use of the new in-situ neutron diffraction cell on Polaris, using Ni-based materials, to illustrate its potential to provide a better understanding of the electrode reactions. In addition, with minor modifications the use of the cell could readily be extended to investigate other type of materials such, as Li- and Na-based electrode materials.

3. Preliminary results on Ni-based batteries

Nickel–metal-hydride (Ni–MH) batteries are widespread in everyday life from small scale applications to hybrid cars and represent the latter development of the nickel-hydrogen battery employed in satellites [22]. Ni–MH batteries use $Ni(OH)_2$ as the positive electrode and hydrogen-absorbing alloy (MH) as the negative electrode. Commercially available electrodes provided by Nilar© were used to evaluate the cell electrochemistry using a LAND CT2001A potentiostat/galvanostat. The cell electrochemistry was initially tested using standard Ni–MH battery components, cell 1, and results compared to deuterated components (electrolyte and separator) which are essential if neutron diffraction patterns with good peak-to-background ratios are to be collected, cell 2. A summary of cell 1 and 2 components is given in Table 1. Cells were cycled galvanostatically at C/12 with cut-off voltages of 1.5/1 V to prevent over-charge/discharge [23] reactions respectively (If such limits are not imposed a potential hazard during the in-situ experiments may occur if the internal pressure of the cell is increased). Electrochemical results are presented in Fig. 2. The cells deliver ≈90% of the specific discharge capacity (mAh g^{-1}) and the voltage versus time plot; inset Fig. 2, shows the typical profile associated with Ni–MH batteries. Small over-potentials are observed in both charge/discharge reactions, i.e. ~1.42 and 1.3 V respectively, which are expected due to the larger dimensions of the cell (e.g. resistance over-potential) compared to typical ex-situ cells or commercially available AAA-sized batteries [24]. This demonstrates that we obtain the expected electrochemical behavior of a Ni–MH battery using our cell when deuterated components, i.e. electrolyte and separator, are used.

Representative neutron diffraction patterns of the cell as a function of discharge state are shown in Fig. 3. The cell was loaded with the MH electrode presented in Table 1 and Ni mesh as counter electrode with 6 M KOD electrolyte and polypropylene (PP) separator. The alloy was first charged ex-situ at a constant current rate of C/12 (41.4 mA) and then discharged in-situ using a lower rate C/17 (29.22 mA) with a cut-off voltage −0.6 V. In Fig. 3, the two most intense peaks correspond to nickel and are due to the cell construction materials i.e. the thin nickel foil used to hold electrodes and the counter electrode. For the fully charged pattern, the remaining reflections can be indexed using a hexagonal unit cell with lattice parameters $a = 5.260(1)$ Å and $c = 4.173(1)$ Å. As discharge proceeds, the intensity of these reflections decrease and other reflections appear that can also be indexed with a hexagonal unit cell but having smaller lattice parameters i.e. $a = 4.995(1)$ Å and $c = 4.040(1)$ Å for the fully discharged state. This corresponds to the β- to α-phase transformation that takes place at the MH electrode during battery discharge [12]. A more detailed investigation of this structural

Table 1
Summary of the components for cell 1 and 2.

Cell type	Positive electrode (Ni electrode)	Negative electrode (MH electrode)	Electrolyte	Separator
Cell 1	$Ni(OH)_2$[a]	$MmNi_{3.6}Al_{0.4}Mn_{0.3}Co_{0.7}$[b]	6 M KOH	Polypropylene (PP)
Cell 2	$Ni(OH)_2$[a]	$MmNi_{3.6}Al_{0.4}Mn_{0.3}Co_{0.7}$[b]	6 M KOD	Polytetrafluoroethylene (PTFE)

[a] Particle size: 90% <25 μm specific capacity (mAh g^{-1}) = 190.
[b] Where Mm = 50–55% La, 30–35% Ce, 9–13% Nd and 3–5% Pr, particle size: 90% <75 μm, specific capacity (mAh g^{-1}) = 270.

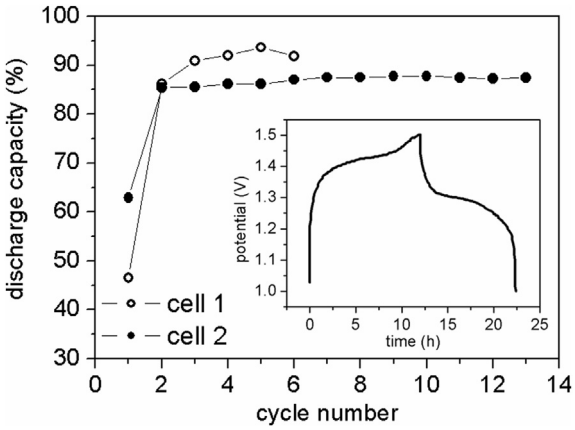

Fig. 2. Electrochemical tests of cell 1 and 2. Cells were cycled galvanostatically at C/12. The discharge capacity versus cycle number is shown and, inset, a representative voltage versus time profile.

transformation will be published elsewhere, however, at this stage; this demonstrates that neutron diffraction data collected in-situ using an Air–MH battery is suitable for monitoring the structural changes at the MH electrode due to the good peak-to-background ratio observed in the diffraction patterns, Fig. 3.

In order to assess the quality of the diffraction data collected using the electrochemical cell presented in this paper, a Rietveld refinement was performed using data collected from the charged state, Fig. 4 and Table 2. The pattern has a small background contribution arising from the PP separator which was modeled in the refinement by using a cosine Fourier series function with 14 variables. The charged MH electrode or β-phase was refined using a $CaCu_5$-type structure (S.G. P6/mmm) [25–28] in which the distribution of metallic atoms was assumed to be the same as the distribution refined in the starting alloy, expressed as the average scattering length per site in Table 2. The Bragg peak profile was

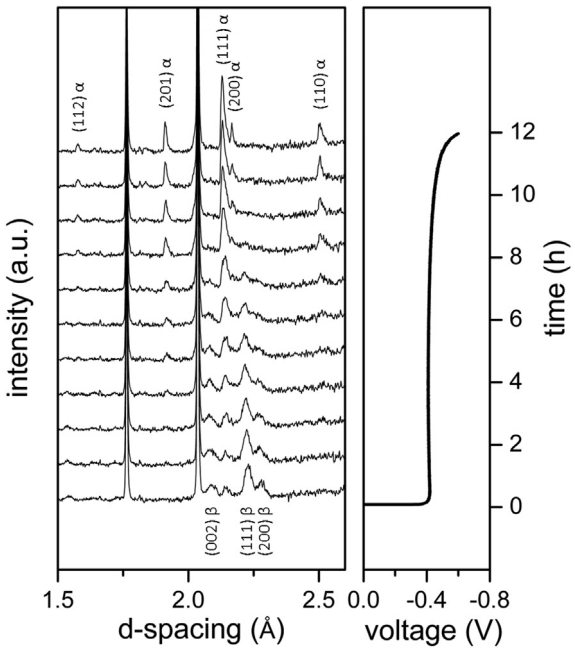

Fig. 3. Neutron diffraction patterns of the cell collected in-situ using the MH electrode (1.84gr) and Ni mesh. Neutron diffraction patterns were collected using 30 min collection times.

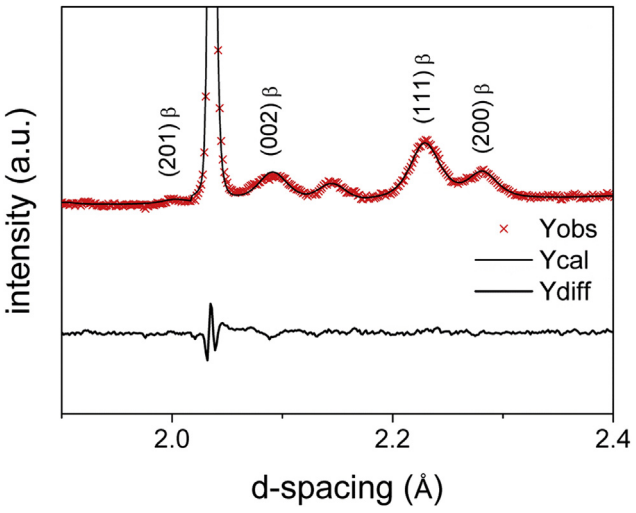

Fig. 4. Fitted neutron diffraction pattern of the cell containing Ni mesh and MH as positive and negative electrodes, respectively. Reflections corresponding to the β-phase are marked.

described using isotropic line widths and this was expected since the anisotropy present in $LaNi_5$ disappears with the substitution of nickel by larger elements such as manganese or aluminum [26]. Initial stages of the refinement included the site occupancy (atom site^{-1}) for deuterium atoms but the structural model did not converge. The deuterium content was then constrained (see formula below) between the available deuterium positions [25] to be 3 D mol^{-1} as obtained from electrochemical results. This allowed the model to converge with a good visual agreement between the model and data and final $\chi^2 = 4.5$

$$(\pm)\delta N_D^{3f} = (\pm)\delta N_D^{4h} = (\pm)\delta N_D^{6m} = (\pm)\delta N_D^{12o} = (\pm)\delta N_D^{12n}$$

Three sites are occupied by deuterium and the site repartition is as follows: D2(6m) > D3(12n) > D1(4h). This agrees well with the site sizes as described by Latroche et al. [26]. The observed Fourier map is presented in Fig. 5. In the $CaCu_5$-type structure, there is a stacking of two different planes at $z = 0$ and $z = 1/2$, with the former containing the 1a, 2c crystallographic sites and the latter the 3g sites. Two distinctive nuclear densities are observed in Fig. 5 which was fitted by the structural model; the 6m Wyckoff site corresponds to the most occupied position of deuterium atoms as obtained by the Rietveld method, Table 2. Therefore, relevant information such as deuterium site preference has been obtained for the β-phase by Rietveld refinement of neutron diffraction data collected from the charged state using the new electrochemical cell.

Table 2
Rieteveld refinement results of the β phase.

Atom	Site	x	y	z	Occupancy*	100 × Uiso (Å^2)
La,Ce,Nd,Pr	1a	0	0	0	6.92 fm	2.37(18)
Ni,Co,Al,Mn	2c	1/3	2/3	0	9.12 fm	3.56(13)
Ni,Co,Al,Mn	3g	1/2	0	1/2	6.93 fm	3.55(11)
D1	4h	1/3	2/3	0.360(6)	0.094(8)	2.5
D2	6m	0.137(1)	0.274(3)	1/2	0.163(6)	2.5
D3	12n	0.464(3)	0	0.080(1)	0.137(4)	2.5

Reliability factors $R_p = 2.04\%$, $R_{wp} = 2.10\%$, $\chi^2 = 4.5\%$.
Charged AB_5-type alloy; AB_5D_3.
S.G. P6/mmm, $a = 5.259(1)$ Å, $b = 5.259(1)$ Å, $c = 4.174(1)$ Å, volume = 100.019(21) Å^3.
* signifies average scattering length per site (fm) or site occupancy (%).

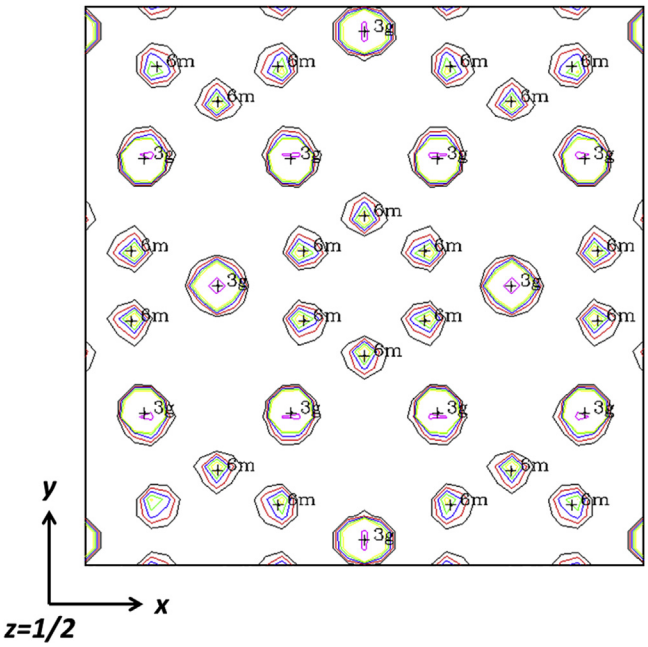

Fig. 5. Observed Fourier map of the β-phase. Contours are drawn at 0.2, 0.4, 0.6, 0.8, 1, 4 and 6. Wyckoff positions 3g and 6m are shown in the map. The deuterium site 6m is the most occupied one, as indicted by the Rietveld analysis.

4. Conclusions

A new electrochemical cell for in-situ neutron diffraction has been designed and successfully tested using Ni-based battery materials on the Polaris diffractometer at the ISIS pulsed neutron source. The cell has a flexible design that allows two configurations to be used dependent on the type of battery technology of interest and the specific aims of a particular experiment. Preliminary results show that the cell delivers the expected electrochemical behavior when tested using $Ni(OH)_2$ and MH as positive and negative electrodes, respectively, with Teflon-based separator and deuterated electrolyte. The structural changes at the MH electrode in a cell containing Ni as a counter electrode have been monitored during discharge in-situ and phase analysis was performed successfully due to the good peak-to-background ratio observed in the neutron diffraction patterns. In addition, detailed structural information such as atomic positions, site occupancies and thermal vibration parameters were refined for the charged MH electrode (β-phase) and the results agree well with previous studies [26,28]. Overall, the cell represents a new opportunity to conduct electrochemical studies in-situ for users at the Polaris diffractometer and it is expected to extend these measurements to other energy materials, e.g. Li-based electrodes, in the near future.

References

[1] L. Eriksson, U. Palmqvist, H. Rundlof, U. Thuresson, R. Sjovall, J. Power Sources 107 (2002) 34–41.
[2] L. Fang, B.V.R. Chowdari, J. Power Sources 97-98 (2001) 181–184.
[3] O. Bergstrom, A.M. Andersson, K. Edstrom, T. Gustafsson, J. Appl. Crystallogr. 31 (1998) 823–825.
[4] Y. Orikasa, T. Maeda, Y. Koyama, H. Murayama, K. Fukuda, H. Tanida, H. Arai, E. Matsubara, Y. Uchimoto, Z. Ogumi, J. Am. Chem. Soc. 135 (2013) 5497–5500.
[5] H. Berg, H. Rundlov, J.O. Thomas, Solid State Ionics 144 (2001) 65–69.
[6] M. Roberts, J.J. Biendicho, S. Hull, P. Beran, T. Gustafsson, G. Svensson, K. Edstrom, J. Power Sources 226 (2013) 249–255.
[7] N. Sharma, V.K. Peterson, M.M. Elcombe, M. Avdeev, A.J. Stunder, N. Blagojevic, R. Yusoff, N. Kamarulzaman, J. Power Sources 195 (2010) 8258–8266.
[8] N. Sharma, G. Du, A.J. Studer, Z. Guo, V.K. Peterson, Solid State Ionics 199-200 (2011) 37–43.
[9] N. Sharma, M.V. Reddy, G. Du, S. Adams, B.V.R. Chowdari, Z. Guo, V.K. Peterson, J. Phys. Chem. C 115 (2011) 21473–21480.
[10] W.R. Brant, S. Schmid, G. Du, N. Sharma, J. Power Sources 244 (2013) 109–114.
[11] M. Latroche, A. Percheron-Guegan, Y. Chabre, C. Poinsignon, J. Pannetier, J. Alloys Compd. 189 (1992) 59–65.
[12] M. Latroche, Y. Chabre, B. Decamps, A. Percheron-Guegan, D. Noreus, J. Alloys Compd. 334 (2002) 267–276.
[13] M. Latroche, A. Percheron-Guegan, Y. Chabre, J. Alloys Compd. 293-295 (1999) 637–642.
[14] M. Latroche, A. Percheron-Guegan, Y. Chabre, J. Bouet, J. Pannetier, E. Ressouche, J. Alloys Compd. 231 (1995) 537–545.
[15] F. Barde, M.R. Palacin, Y. Chabre, O. Isnard, J.-M. Tarascon, Chem. Mater. 16 (2004) 3936–3948.
[16] W. Peng, L. Redey, A.N. Jansen, D.R. Vissers, K.M. Myles, J.M. Carpenter, J.W. Richarson, G.L. Burr, J.R. Selman, J. Electrochem. Soc. 144 (11) (1997) 3836–3844.
[17] F. Rosciano, M. Holzapfel, W. Scheifele, P. Novak, J. Appl. Crystallogr. 41 (2008) 690–694.
[18] J.-F. Colin, V. Godbole, P. Novak, Electrochem. Commun. 12 (2010) 804–807.
[19] V.A. Godbole, M. He, C. Villevieille, H. Kaiser, J.-F. Colin, P. Novak, RSC Adv. 3 (2013) 757–763.
[20] A.C. Larson, R.B. Von Dreele, Report LA-UR-86–748, Los Alamos National Laboratory, Los Alamos, 1990, NM87545.
[21] S. Hull, R.I. Smith, W.I.F. David, A.C. Hannon, J. Mayers, R. Cywinski, Phys. B 180–181 (1992) 1000–1002.
[22] R.M. Dell, D.A.J. Rand, Understanding Batteries, RSC, 2001.
[23] K. Hong, J. Alloys Compd. 321 (2001) 307–313.
[24] T.-K. Ying, X.-P. Gao, W.-K. Hu, F. Wu, D. Noréus, Int. J. Hydrogen Energy 31 (2006) 525–530.
[25] A. Percheron-Guegan, C. Lartigue, J.C. Achard, P. Germi, F. Tasset, J. Less-Common Met. 74 (1980) 1–12.
[26] M. Latroche, J. Rodriguez-Carvajal, A. Percheron-Guegan, F. Bouree-Vigneron, J. Alloys Compd. 218 (1995) 64–72.
[27] J.-M. Joubert, R. Cerny, M. Latroche, A. Percheron-Guegan, K. Yvon, J. Appl. Crystallogr. 31 (1998) 327–332.
[28] P.A. Georgiev, J. Liu, D.K. Ross, H.H. Andersen, A. Otto, J. Alloys Compd. 349 (2003) 325–333.